Probing the electronic band structure of ferromagnets with spin injection and extraction

Pawel Bruski,[1] Steven C. Erwin,[2] Jens Herfort,[1] Abbes Tahraoui,[1] and Manfred Ramsteiner[1,*]
[1]*Paul-Drude-Institut für Festkörperelektronik, Hausvogteiplatz 5–7, 10117 Berlin, Germany*
[2]*Center for Computational Materials Science, Naval Research Laboratory, Washington, DC 20375, USA*
(Received 11 September 2014; revised manuscript received 12 December 2014; published 31 December 2014)

We study spin injection and spin extraction signals in lateral spin-valve structures consisting of ferromagnetic Co_2FeSi contacts on n-type GaAs transport channels. The dependence of the spin-valve signals on the bias current is found to strongly depend on the degree of ordering in the Co_2FeSi lattice. For the fully ordered $L2_1$ phase, the signal is equal for injection and extraction and independent of the bias current. In contrast, a strong dependence of the relative signal strengths (spin injection versus extraction) on the bias current is observed for the partially disordered $B2$ phase. We explain the strongly different behavior by the crucial influence of the respective electronic band structure on the spin generation processes.

DOI: 10.1103/PhysRevB.90.245150 PACS number(s): 72.25.Mk, 75.76.+j, 72.25.Dc, 75.50.Bb

I. INTRODUCTION

For semiconductor spintronics, the generation of spin-polarized carriers in nonmagnetic semiconductors by electrical means is regarded as a major building block [1]. One promising approach to realize such building blocks is the utilization of ferromagnetic contacts acting as spin-polarized sources in ferromagnet/semiconductor (FM/SC) or FM/insulator/SC hybrid structures. Two processes are considered for the generation of a spin accumulation in the SC when driving an electrical current through the interface(s). For n-type SCs, spin injection refers to the case of a net electron flow from the FM into the SC (reverse bias for Schottky contacts). In contrast, an electron flow from the SC into the FM (forward bias for Schottky contacts) leads to the process of spin extraction, resulting in a spin polarization in the SC which is of opposite sign compared to that created by spin injection [2,3]. In a nonlocal spin valve (NLSV) consisting of FM contact strips on a nonmagnetic (n-type SC, metal, graphene) lateral transport channel, both spin generation processes can be observed [3–12]. Nonlinear dependences of the NLSV signals on the bias current were discussed in some reports in terms of an exchange-split energy band in the FM assuming a parabolic dispersion [10], or localized electron states near (at) the FM/SC interface [4,5,9,13].

We have previously demonstrated that the hybrid system consisting of the Heusler alloy Co_2FeSi on n-type GaAs transport channels holds promise for potential spintronic applications [3,14]. Co_2FeSi in the fully ordered $L2_1$ phase is considered to be half metallic and, hence, an ideal candidate for electrical spin injection [15]. Disorder drastically modifies the electronic band structure [16]. The partially disordered $B2$ phase, for example, not only lacks half metallicity, but also exhibits an opposite spin polarization at the Fermi level. In this paper, we investigate the bias-current dependence of spin generation in Co_2FeSi/GaAs NLSVs and compare our experimental results with the expectations derived from the bulk band structures obtained by first-principles calculations for the two different Co_2FeSi phases.

II. EXPERIMENT

The investigated samples were grown by molecular beam epitaxy on semi-insulating GaAs(001) substrates. The layer sequence consists of a 1500-nm-thick, lightly n-type doped ($n_L = 2 \times 10^{16}$ cm^{-3}) GaAs spin transport layer, followed by a 15-nm-thick layer with a linearly increasing doping density ranging from n_L to $n_H = 5 \times 10^{18}$ cm^{-3} and a heavily doped (n_H) 15-nm-thick layer leading to a narrow Schottky barrier. After transfer in ultrahigh vacuum into a growth chamber for metals, a 16-nm-thick layer of the ferromagnetic Heusler alloy Co_2FeSi was deposited epitaxially. Detailed information on the growth of the Heusler alloy Co_2FeSi is provided elsewhere [17,18]. Most important for our investigation is the fact that the crystal phase in the Co_2FeSi layers can be controlled by the choice of the appropriate substrate temperature (T_S) during growth [16,19,20]. Layers consisting dominantly of the $L2_1$ ($B2$) phase were grown at $T_S = 280\,^\circ$C ($T_S \approx 60\,^\circ$C).

The lateral transport devices were processed by wet chemical etching as well as photolithography, and finally by the evaporation of Au bond pads. The device structure comprises a 50×400 μm^2 conductive mesa region with Co_2FeSi strip contacts and is described in more detail in Ref. [14]. For the present experiments, a center-to-center separation between the spin generation (injection or extraction) and detection contact strips was chosen to lie between 6.5 and 12.5 μm. All measurements were performed at 20 K in a He exchange gas cryostat with the electrical signals recorded by a standard dc method. The NLSV experiments were conducted in the same manner as described, e.g., in Refs. [4,6,14].

III. RESULTS AND DISCUSSION

A. Spin-valve signals

The operation of NLSVs containing $L2_1$ Co_2FeSi contact strips has already been demonstrated in Ref. [14]. For a NLSV structure with $B2$ Co_2FeSi contact strips, the absolute value of the nonlocal spin voltage (V_{NL}) is shown in Fig. 1 as a function of the external magnetic field ($\mu_0 H$) for the two opposite bias-current directions. The observed voltage jumps ΔV_{inj} and ΔV_{extr} correspond to the switching between parallel and antiparallel magnetization of the spin generating and detecting strips during an upward sweep of the magnetic field. These

*ramsteiner@pdi-berlin.de

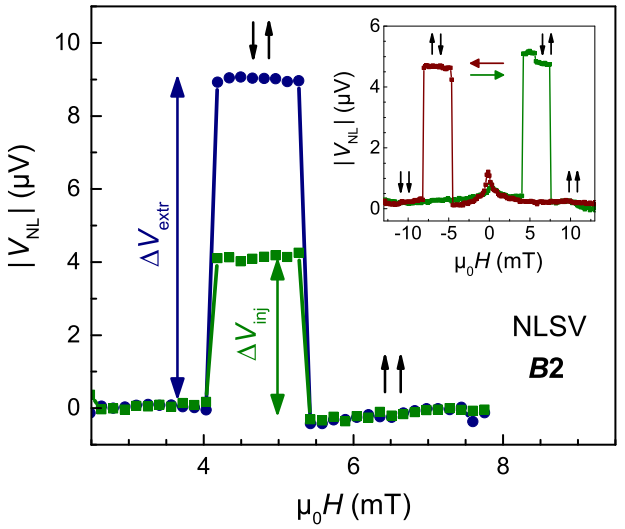

FIG. 1. (Color online) Absolute value of the nonlocal voltage V_{NL} as a function of an external magnetic field ($\mu_0 H$) for a spin-valve structure with $B2$-phase Co_2FeSi contacts and an absolute bias current of 200 μA. The NLSV signals obtained during an upward sweep of the magnetic field are shown for both a net electron flow into (dark blue circles: ΔV_{extr}) and out of (green squares: ΔV_{inj}) the contact strip used for spin generation. Note that the V_{NL} jumps for spin extraction and injection are of opposite sign. ΔV_{extr} and ΔV_{inj} are defined as their absolute values. Inset: NLSV signal induced by spin injection during upward and downward sweeps of the magnetic field.

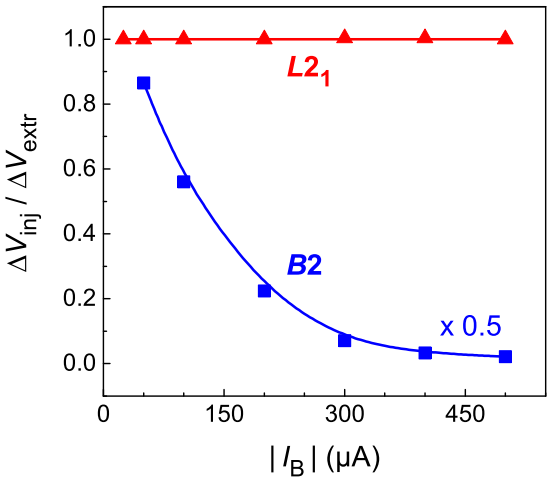

FIG. 2. (Color online) Ratio of the NLSV signals obtained under spin injection (ΔV_{inj}) and spin extraction (ΔV_{extr}) conditions as a function of the absolute value of the current. Data are shown for Co_2FeSi contact strips consisting dominantly of either the $L2_1$ or the $B2$ phase. Note that the $\Delta V_{inj}/\Delta V_{extr}$ values for the $B2$-phase contacts are shown with a scaling-down factor of 0.5. The solid lines are guides to the eye.

characteristic spin-valve signatures provide clear evidence for both electrical injection and extraction of spin-polarized electrons in Co_2FeSi/GaAs transport structures. Note that the V_{NL} jumps for spin extraction and injection are actually of opposite sign. ΔV_{extr} and ΔV_{inj} are defined as their absolute values. The complete NLSV characteristics including both upward and downward sweeps of the magnetic field is shown in the inset of Fig. 1 for the case of spin injection using $B2$ contact strips. The same types of characteristic V_{NL} jumps have been observed for all NLSV structures. It is worth noting that the determination of the spin generation efficiencies along the lines of Ref. [14] results in values clearly below 100% for both $L2_1$- and $B2$-phase contacts. However, the underlying analysis contains assumptions of unknown validity [14]. Furthermore, spin relaxation processes in the proximity of the FM/SC interface, e.g., due to magnetic fringe fields induced by interface roughnesses, are not taken into account [9,21,22]. Consequently, even for half-metallic contacts the extracted spin generation efficiencies are not expected to reveal the ultimate magnitude. However, the observed injection signal (ΔV_{inj}) is significantly different from the spin extraction signal (ΔV_{extr}) at the same absolute value of the bias current (200 μA). In contrast, for NLSVs with $L2_1$ contact strips, ΔV_{inj} and ΔV_{extr} have been found to be nearly identical under the same conditions.

Figure 2 shows the ratio of the two signals $\Delta V_{inj}/\Delta V_{extr}$ for Co_2FeSi contact strips consisting dominantly of either the $L2_1$ or the $B2$ phase as a function of the absolute value of the bias current. For the spin generation induced by $B2$-phase contacts, $\Delta V_{inj}/\Delta V_{extr}$ clearly decreases with increasing absolute value of the current. Thereby, the injection signal exceeds the extraction signal ($\Delta V_{inj}/\Delta V_{extr} > 1$) at the lowest current values (note the downscaling of the data by a factor of 0.5). In contrast, for a NLSV with contact strips consisting of the $L2_1$ phase, the spin injection and extraction signals are of the same magnitude, i.e., the ratio $\Delta V_{inj}/\Delta V_{extr}$ remains exactly at unity.

B. Current-voltage characteristics

To clarify whether or not the electrical Co_2FeSi/GaAs contact properties are the origin of the different behavior found for the spin generation induced by the $B2$ and $L2_1$ phases (cf. Fig. 2), we measured the current-voltage characteristics of the respective contacts in a three-terminal arrangement described, e.g., in Ref. [23]. The obtained voltage drop at the FM/SC interface (V_B) is shown in Fig. 3 as a function of bias current (I_B) for $L2_1$- and $B2$-phase contacts. Both current-voltage curves are not fully symmetric with respect the forward and reverse current directions, i.e., for spin extraction and injection conditions, respectively. However, the observed asymmetries are very similar for $L2_1$- and $B2$-phase contacts. Consequently, we exclude the electrical contact properties as the major reason for the strongly different current dependences of $\Delta V_{inj}/\Delta V_{extr}$ observed for $L2_1$ and $B2$ Co_2FeSi contacts (cf. Fig. 2). Nevertheless, it is worth noting that the asymmetry in the current-voltage curve is presumably the reason for $\Delta V_{inj}/\Delta V_{extr}$ being larger than unity at the lowest current values in the case of $B2$-phase contacts (cf. Fig. 2). The signal ratios shown in Fig. 2 have been determined at fixed absolute current values which correspond to somewhat different interface voltages V_B in forward (extraction) and reverse (injection) directions. For example, a fixed bias current of 100 μA corresponds to interface voltages of 218 and 285 mV in the forward and reverse directions, respectively (cf. Fig. 3).

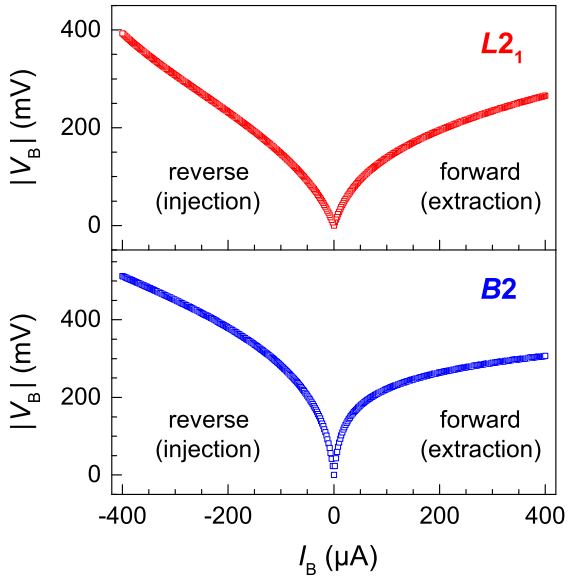

FIG. 3. (Color online) Absolute value of the FM/SC interface voltage (V_B) as a function of the bias current measured in a three-terminal arrangement for $L2_1$- and $B2$-phase Co_2FeSi contacts.

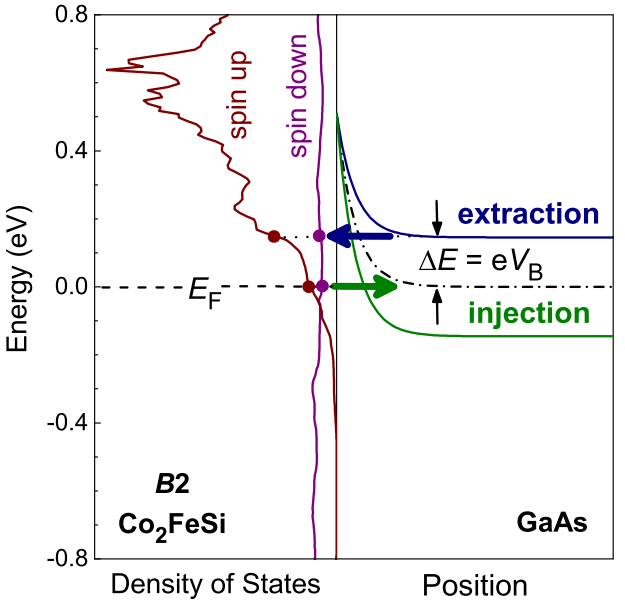

FIG. 4. (Color online) Left panel: Spin-dependent (spin-up and spin-down) density of states for the $B2$ phase of Co_2FeSi obtained by first-principles calculations [16]. Right: Conduction band edge in GaAs as a function of position for the cases of spin injection (lower green curve) and spin extraction (upper dark blue curve) conditions. The directions of the net electron flow are indicated by the dark blue leftwards and green rightwards arrows for spin injection and spin extraction conditions, respectively.

However, for $B2$-phase contacts, the individual signals ΔV_{inj} and ΔV_{extr} depend in a very different manner on the interface voltage V_B, as will be shown in the discussion below.

C. Simulation of spin generation

In order to understand the strongly different behavior of the two Co_2FeSi phases revealed in Fig. 2, we have to consider the bias voltage dependence of the spin generation processes with regard to the specific electronic band structure in the ferromagnetic contacts. The two different spin generation processes, spin injection and extraction, are illustrated in Fig. 4 and have to be distinguished in the following way. The transmission of free carriers through a FM/SC interface is spin dependent for either direction of the electrical current due to the spin-dependent density of states (DOS) in the conduction band of the FM. Spin injection (reverse bias) takes place mainly at the (quasi-) Fermi energy (E_F) in the FM, considering tunneling through the Schottky barrier being much less efficient for electrons at lower energies. In a more accurate approach, we include the contribution of electron states at energies (E) below the Fermi level in Co_2FeSi and use the following low-temperature approximation for the transmission coefficients of spin-up ($T^{\uparrow}$) and spin-down ($T^{\downarrow}$) electrons at the FM/SC interface:

$$T^{\uparrow,\downarrow}(\Delta E) \propto \int_{E_F-\Delta E}^{E_F} W(E) D^{\uparrow,\downarrow}(E) dE, \tag{1}$$

where $D^{\uparrow,\downarrow}(E)$ is the spin-dependent density of states in the Co_2FeSi conduction band (see the left panel of Fig. 4 for the $B2$ phase). The quasi-Fermi level E_F on the FM side is chosen as the point of reference for the energy scale ($E = 0$). As a tunneling weighting factor, we use $W(E) = \exp[-(\Phi_B - E)/E_0]$ with reasonable values for the Schottky barrier heigtht $\Phi_B = 0.7$ eV and the characteristic tunneling energy $E_0 = 0.1$ eV. In the lightly doped semiconductor channel, a very narrow (δ-like) energy distribution of occupied states is assumed with the Fermi energy lying only a few meV above the conduction band edge.

For spin extraction (forward bias), we have to consider the DOS in the FM at an energy $\Delta E = eV_B$ above the (quasi-) Fermi energy (cf. Fig. 4). Finally, we arrive at following relations for the spin polarizations P_{inj} and P_{extr} created in the semiconductor by spin injection and extraction, respectively:

$$P_{inj}(\Delta E) \propto \frac{T^{\uparrow}(\Delta E) - T^{\downarrow}(\Delta E)}{T^{\uparrow}(\Delta E) + T^{\downarrow}(\Delta E)} \underset{\sim}{\propto} \Pi(E_F), \tag{2}$$

$$P_{extr}(\Delta E) \propto \Pi(E_F + \Delta E), \tag{3}$$

$$\Pi(E) = \frac{D^{\uparrow}(E) - D^{\downarrow}(E)}{D^{\uparrow}(E) + D^{\downarrow}(E)}. \tag{4}$$

In fact, both the injected and extracted spin polarizations depend in a combined manner on the voltage $V_B = \Delta E/e$ and the energy-dependent spin polarization $\Pi(E)$ in the conduction band of Co_2FeSi. Since the NLSV signals (ΔV_{inj} and ΔV_{extr}) are both proportional to the generated spin polarizations in the SC (P_{inj} and P_{extr}), we use the following relations for the comparison between experiment and simulation (see, e.g., Ref. [14]),

$$\Delta V_{inj(extr)} = \gamma P_{inj(extr)} I_B, \tag{5}$$

$$\frac{\Delta V_{inj}}{\Delta V_{extr}} = \frac{P_{inj}}{P_{extr}}, \tag{6}$$

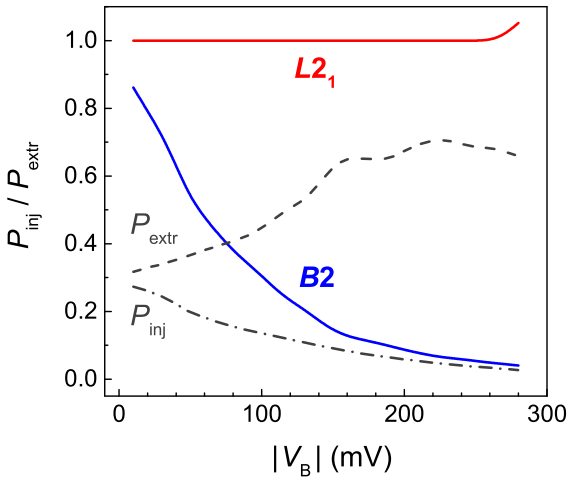

FIG. 5. (Color online) Calculated ratio of the injected and extracted spin polarizations P_{inj}/P_{extr} as a function of the absolute value of $V_B = \Delta E/e$ for both phases ($L2_1$ and $B2$) of Co_2FeSi. For the $B2$ phase, the polarizations P_{inj} (dashed-dotted) and P_{extr} (dashed) are also shown separately. Note that the current I_B applied during NLSV experiments is a monotonic (but nonlinear) function of the voltage V_B.

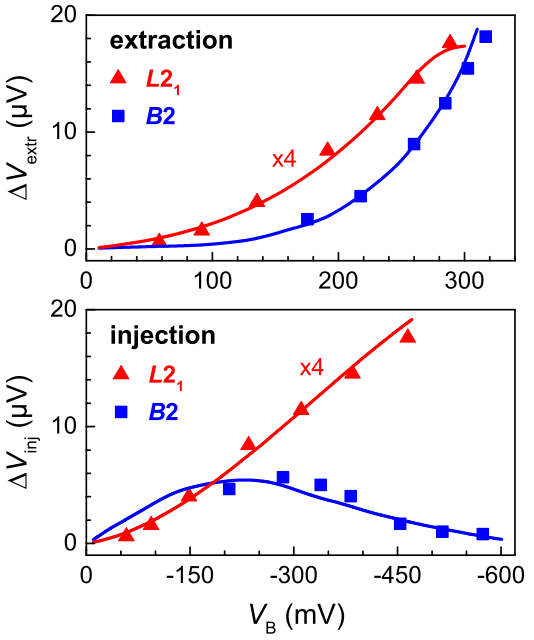

FIG. 6. (Color online) Measured (symbols) and calculated (solid lines) spin signals (ΔV_{inj} and ΔV_{extr}) under spin extraction (upper panel) and injection (lower panel) conditions as a function of the interface voltage V_B for both $L2_1$ (triangles) and $B2$ (squares) Co_2FeSi contacts. Note that the ΔV_{inj} and ΔV_{extr} values for the $L2_1$-phase contacts are shown with a scaling-up factor of 4.

where γ represents a constant (bias-independent) factor for a given NLSV configuration. For the calculation of P_{inj} and P_{extr} based on Eqs. (1)–(3), we used the spin-dependent density of states $D^{\uparrow,\downarrow}(E)$ of Co_2FeSi given in Ref. [16] as a result of first-principles calculations (see the left panel of Fig. 4 for the $B2$ phase).

Figure 5 displays the simulated ratios P_{inj}/P_{extr} as a function of the absolute value of the voltage $V_B = \Delta E/e$ for both the $L2_1$ and the $B2$ phase. Because of the half-metallic characteristic of the $L2_1$ phase, the spin polarization $\Pi(E)$ is 100% in the vicinity of the Fermi energy resulting in constant polarizations $P_{inj} = P_{extr} = 1$ as well as a constant ratio $P_{inj}/P_{extr} = 1$ in almost the whole energy range between 0 and 300 meV. In contrast, for the $B2$ phase, the injected (extracted) spin polarization P_{inj} (P_{extr}) decreases (increases) with increasing voltage $V_B = \Delta E/e$. As a consequence, the ratio P_{inj}/P_{extr} exhibits a strong energy (voltage) dependence. The qualitative behavior obtained for $B2$-phase contacts can be easily deduced from the corresponding electronic band structure shown in Fig. 4. For the $L2_1$ phase, the spin-dependent density of states is given in Ref. [16]. The band structure obtained by first-principles calculations reveals a half-metallic gap which extends from 800 meV below to about 300 meV above the Fermi energy. As a consequence, the polarization P_{extr} starts to decrease when approaching $V_B = 300$ mV ($\Delta E = 300$ meV), which is manifested in Fig. 5 by an increase in the ratio P_{inj}/P_{extr}. Since the voltage V_B is a monotonic function of the current applied during the NLSV experiments (cf. Fig. 3), it is justified to directly compare the experimental data in Fig. 2 with the simulated results in Fig. 5. Indeed, the simulated voltage (current) dependence of P_{inj}/P_{extr} (cf. Fig. 5) reproduces the strong difference in the behavior of the NLSV signal ratio $\Delta V_{inj}/\Delta V_{extr}$ observed for the two Co_2FeSi phases (cf. Fig. 2). In contrast to the simulation for $L2_1$-phase contacts, the measured signal ratio exhibits no increase when approaching $V_B = 300$ mV. This finding indicates that the actual half-metallic gap extends to even more than 300 meV above the Fermi energy. Note that a constant ratio P_{inj}/P_{extr} (or $\Delta V_{inj}/\Delta V_{extr}$) could also be obtained by a ferromagnetic band structure with exactly the same energy dependence of a finite density of states for both spin subsystems (above and below the Fermi level) which, however, constitutes an extremely unlikely case.

In order to directly compare our simulations with the measured NLSV data, we display in Fig. 6 the individual signals ΔV_{inj} and ΔV_{extr} as a function of the interface voltage V_B. For the simulations according to Eq. (5) as well as for the presentation of the experimental data, the relation between the bias current I_B and the interface voltage V_B has been taken from the current-voltage curves shown in Fig. 3. Note that the absolute signal strengths depend on the actual device dimensions chosen for the NLSV measurements with the $L2_1$- or $B2$-phase contacts. For the voltage dependences of all individual NLSV signals, a good agreement is found between experiment and simulation. In the case of $B2$-phase contacts, different scaling factors γ have to be used for injection and extraction conditions in order to account for the experimentally observed relative signal strengths. Most strikingly, the spin injection signals of the two different Co_2FeSi phases reveal strongly different voltage dependences. Remarkably, no decrease of the spin injection signal ΔV_{inj} is observed for voltages up to 450 mV in the case of $L2_1$-phase contacts. This finding indicates that voltage-dependent spin relaxation processes in the GaAs channel under reverse-bias conditions are here of minor importance [9,22].

IV. CONCLUSIONS

Our observations demonstrate that the specific characteristics of the electronic band structures in the FM contacts indeed manifest themselves in the current dependences of the spin generation processes. With this knowledge, we have a tool at hand to probe details of the spin-polarized electronic band structure of ferromagnetic materials. In this way, our experimental findings confirm the results of the first-principles calculations reported in Ref. [16]. In particular, for the $L2_1$ phase of Co_2FeSi, the prediction of a half-metallic character is strongly supported, an important material property which is otherwise very difficult to access experimentally.

ACKNOWLEDGMENTS

We acknowledge the expert technical support by Walid Anders, Angela Riedel, and Gerd Paris, as well as the critical reading of the manuscript by Oliver Brandt and Holger Grahn. This work was supported in part by the U.S. Office of Naval Research Laboratory's Basic Research Program.

[1] E. Y. Tsymbal and I. Zutic, *Handbook of Spin Transport and Magnetism* (Chapman and Hall/CRC, London, 2011).
[2] V. V. Osipov and A. M. Bratkovsky, Phys. Rev. B **72**, 115322 (2005).
[3] Y. Manzke, R. Farshchi, P. Bruski, J. Herfort, and M. Ramsteiner, Phys. Rev. B **87**, 134415 (2013).
[4] X. Lou, C. Adelmann, S. A. Crooker, E. S. Garlid, J. Zhang, K. S. M. Reddy, S. D. Flexner, C. J. Palmstrøm, and P. A. Crowell, Nat. Phys. **3**, 197 (2007).
[5] A. N. Chantis, K. D. Belashchenko, D. L. Smith, E. Y. Tsymbal, M. van Schilfgaarde, and R. C. Albers, Phys. Rev. Lett. **99**, 196603 (2007).
[6] M. Ciorga, A. Einwanger, U. Wurstbauer, D. Schuh, W. Wegscheider, and D. Weiss, Phys. Rev. B **79**, 165321 (2009).
[7] O. M. J. van't Erve, C. Awo-Affouda, A. T. Hanbicki, C. H. Li, P. E. Thompson, and B. T. Jonker, IEEE Trans. Electron Devices **56**, 2343 (2009).
[8] Y. Ando, K. Kasahara, K. Yamane, K. Hamaya, K. Sawano, T. Kimura, and M. Miyao, Appl. Phys. Express **3**, 093001 (2010).
[9] G. Salis, S. F. Alvarado, and A. Fuhrer, Phys. Rev. B **84**, 041307(R) (2011).
[10] S. O. Valenzuela, D. J. Monsma, C. M. Marcus, V. Narayanamurti, and M. Tinkham, Phys. Rev. Lett. **94**, 196601 (2005).
[11] F. Casanova, A. Sharoni, M. Erekhinsky, and I. K. Schuller, Phys. Rev. B **79**, 184415 (2009).
[12] N. Tombros, C. Jozsa, M. Popinciuc, H. T. Jonkman, and B. van Wees, Nature (London) **448**, 571 (2007).
[13] H. Dery and L. J. Sham, Phys. Rev. Lett. **98**, 046602 (2007).
[14] P. Bruski, Y. Manzke, R. Farshchi, O. Brandt, J. Herfort, and M. Ramsteiner, Appl. Phys. Lett. **103**, 052406 (2013).
[15] R. Farshchi and M. Ramsteiner, J. Appl. Phys. **113**, 191101 (2013).
[16] P. Bruski, S. C. Erwin, M. Ramsteiner, O. Brandt, K.-J. Friedland, R. Farshchi, J. Herfort, and H. Riechert, Phys. Rev. B **83**, 140409(R) (2011).
[17] M. Hashimoto, J. Herfort, H.-P. Schönherr, and K. H. Ploog, Appl. Phys. Lett. **87**, 102506 (2005).
[18] M. Hashimoto, J. Herfort, H.-P. Schönherr, and K. H. Ploog, J. Appl. Phys. **98**, 104902 (2005).
[19] M. Hashimoto, A. Trampert, J. Herfort, and K. H. Ploog, J. Vac. Sci. Technol. B **25**, 1453 (2007).
[20] B. Jenichen, J. Herfort, T. Hentschel, A. Nikulin, X. Kong, A. Trampert, and I. Žižak, Phys. Rev. B **86**, 075319 (2012).
[21] S. P. Dash, S. Sharma, J. C. Le Breton, J. Peiro, H. Jaffrès, J.-M. George, A. Lemaître, and R. Jansen, Phys. Rev. B **84**, 054410 (2011).
[22] M. W. Wu, J. H. Jiang, and M. Q. Weng, Phys. Rep. **493**, 61 (2010).
[23] T. Uemura, K. Kondo, J. Fujisawa, K.-I. Matsuda, and M. Yamamoto, Appl. Phys. Lett. **101**, 132411 (2012).